A truly hyperbolic elastic metamaterial lens

Joo Hwan Oh, Hong Min Seung, and Yoon Young Kim

Citation: Applied Physics Letters **104**, 073503 (2014); doi: 10.1063/1.4865907
View online: http://dx.doi.org/10.1063/1.4865907
View Table of Contents: http://scitation.aip.org/content/aip/journal/apl/104/7?ver=pdfcov
Published by the AIP Publishing

A truly hyperbolic elastic metamaterial lens

Joo Hwan Oh, Hong Min Seung, and Yoon Young Kim[a)]
WCU Multiscale Design Division, School of Mechanical and Aerospace Engineering, Seoul National University, 599 Gwanak-ro, Gwanak-gu, Seoul 151-744, South Korea

(Received 18 November 2013; accepted 3 February 2014; published online 18 February 2014)

Sub-wavelength imaging is possible if metamaterial lenses realizing hyperbolic or elliptic Equi-Frequency Contours (EFCs) are used. Theoretically, lenses exhibiting hyperbolic EFCs allow imaging with unlimited resolution, but only metamaterials of elliptic EFCs producing limited resolution have been so far realized in elastic field. Thus, an elastic metamaterial lens realizing truly hyperbolic EFCs can lead to superior-resolution ultrasonic imaging. This Letter presents the realization of an elastic lens exhibiting truly hyperbolic EFCs and its experimental verification.
 [http://dx.doi.org/10.1063/1.4865907]

As we pursue sub-wavelength imaging by using a magnifying elastic metamaterial lens realizing hyperbolic EFCs, we begin with Fig. 1 that compares hyperbolic[1–8] and elliptic[9–12] EFCs. Because image details are decomposed along the θ direction, higher-resolution sub-wavelength imaging is possible if wave components of large circumferential wave numbers (k_θ's) can propagate along the r direction.[13,14] Compare elliptic and hyperbolic EFCs in Fig. 1; it is apparent that virtually unlimited resolution can be possible only if a hyperbolic EFC is used; in case of an elliptic EFC, however, any information contained in k_θ's larger than $\hat{k}_\theta$ cannot be carried along the r direction because there exists no propagating wave beyond $k_\theta = \hat{k}_\theta$. In case of elastic or acoustic media, metamaterial lens realizing only elliptic EFCs have been so far realized.[9,10,12] Although these lenses, commonly called hyperlens, are capable of sub-wavelength imaging due to strong anisotropy in the elliptic EFC, further resolution improvement cannot be possible unless a lens realizing hyperbolic EFCs is used.

The issue is how to realize an elastic metamaterial having hyperbolic EFCs. We argue that the reason for no realization of a hyperbolic elastic lens so far, unlike in the electromagnetic field,[1–7] is due to lack of utilization of various elastic deformation modes such as extension, bending, and shearing that are generally coupled with each other. In electromagnetic or acoustic fields, only the same type of wave modes is present in comparison with elastic waves. Therefore, metamaterial design with elastic media may be more difficult but on the other hand, the availability of various deformation modes gives more freedom in making metamaterial unit cells. With this in mind, let us first summarize the underlying criteria that an elastic hyperbolic metamaterial lens should satisfy.

Referring to Fig. 1, waves should propagate only along the r direction, not along the θ direction for a selected frequency to have a hyperbolic EFC. Another condition to consider is that the size of a unit cell in a metamaterial should be much smaller than the working wavelength in a host material. If this condition is not met as in phononic crystals,[15,16] transmitted waves from a metamaterial may be scattered into various directions.[17] Finally, the size of a unit cell larger than 1 cm may be preferred to facilitate metamaterial fabrication by a conventional machining process, making the operating frequency as low as 10 kHz. Note that a metamaterial using resonance[8,11,18,19] will not be used here because it usually suffers from high loss and operates in a very narrow frequency range.[9]

Let us now consider a mass-spring model illustrated in Fig. 2(a) which is supposed to simulate an elastic metamaterial to be engineered. To forbid wave propagation along the θ direction, our idea is to add a mass m_2 acting mainly in the θ direction and a soft spring s_2 (such that $s_2 \ll s_1$). Because m_2 is added serially to m_1, there will be developed a bandgap frequency zone where no wave propagates along the θ direction while there is always a propagating wave in the r direction. For more detailed analysis procedure, see supplementary material.[20] Since s_2 is serially connected to s_1, s_2 ($s_2 \ll s_1$) predominantly determines the overall stiffness in the θ direction, making the wave speed in the θ direction much slower than the wave speed in the r direction (in a propagating frequency band). If the operating frequency is above a certain value, the proposed mass-spring model can exhibit hyperbolic EFCs as in Fig. 2(b). Recall that earlier attempts to use extreme anisotropy for acoustic[9,10] and elastic[12] sub-wavelength imaging used elliptic EFCs, not hyperbolic EFCs.

It is worth mentioning that the advantage of the proposed mass-spring model is that the circumferential and radial wave motions are controlled independently from each other because of the introduction of s_2 among others; thus,

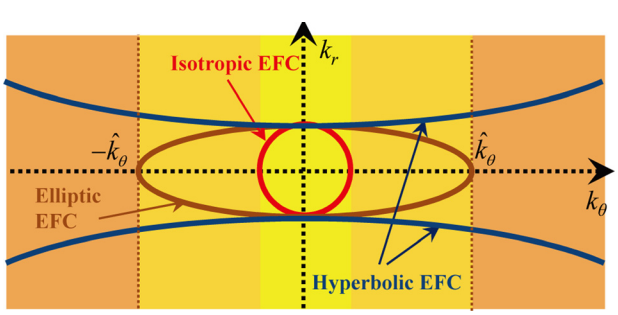

FIG. 1. Comparison between EFCs of a general isotropic material and elliptic/hyperbolic EFCs.

[a)]Author to whom correspondence should be addressed. Electronic mail: yykim@snu.ac.kr. Tel.: +82-2-880-7154. FAX: +82-2-872-1513.

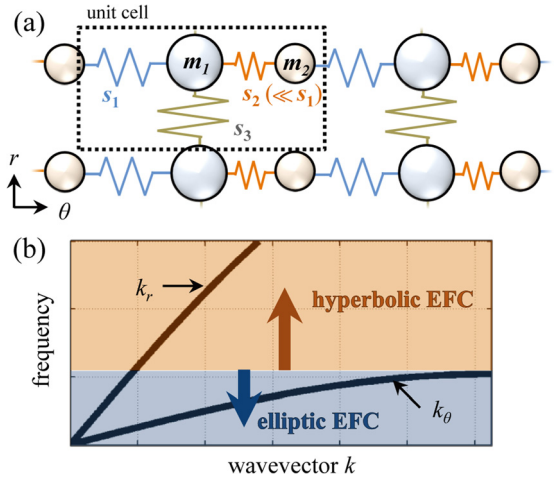

FIG. 2. (a) A two-dimensional discrete mass-spring model for engineering an elastic metamaterial lens exhibiting truly hyperbolic EFCs. (b) Schematic dispersion curves for the mass-spring model in (a). Note that only acoustic branches are plotted in this figure.

engineering of structural layouts of the corresponding metamaterial may be better facilitated than any model exhibiting fully coupled motions.

Fig. 3(a) shows the actual metamaterial realization equivalent to the mass-spring model in Fig. 2(a). In this model, the mass of segment S_1 is m_1, while the mass of segment S_2 is m_2. The stiffness of segment S_1 in the θ and r directions are s_1 and s_3, respectively, while the stiffness of segment S_2 is s_2. The key in the proposed metamaterial is to introduce Segment S_2 that is flexible in one direction. Because the stiffness of the proposed structure S_2 in the θ direction is much smaller than that in the r direction, the segment provides flexibility along the θ direction. The coefficients m_1, m_2, s_1, s_2, and s_3 are related to the material properties and geometric variables of Segments S_1 and S_2 as[21]

$$m_1 = \rho V_{S_1},\ m_2 = \rho V_{S_2}, \tag{1a}$$

$$s_1 = Eh_{S_1}t_{S_1}/[l_{S_1}(1-\nu^2)],\quad s_2 = f(\alpha_{S_2}, \beta_{S_2}, \gamma_{S_2}),$$
$$s_3 = El_{S_1}t_{S_1}/h_{S_1}. \tag{1b}$$

In Eq. (1a), V_{S_1} and V_{S_2} are the volumes of Segments S_1 and S_2 and in Eq. (1b), variables subscribed by S_1 and S_2 denote the geometrical variables of Segments S_1 and S_2, respectively. See supplementary material for the definition of the variables and the derivation of s_1, s_2, and s_3.[20]

The unit cell in Fig. 3(a) may appear to resemble the acoustic coiling-up structures,[22–24] but the proposed structure cannot be explained by wave path elongation. Unlike acoustics, the different deformation mechanisms along the two different directions are responsible to produce hyperbolic EFCs in the present elastic case.

Let us examine the metamaterial lens to realize hyperbolic EFCs in more detail. The lens is fabricated on a 1 mm-thick aluminum plate. While the metamaterial will work in a considerably large range of frequencies (as no resonance is used), the target frequency is selected to be 15 kHz in engineering a hyperbolic lens. For the fabrication, we begin to fill the innermost region of the lens with unit cells of $w = 9.6$ mm and $\Delta\theta = 2.74°$. Obviously, unit cells have the same w and

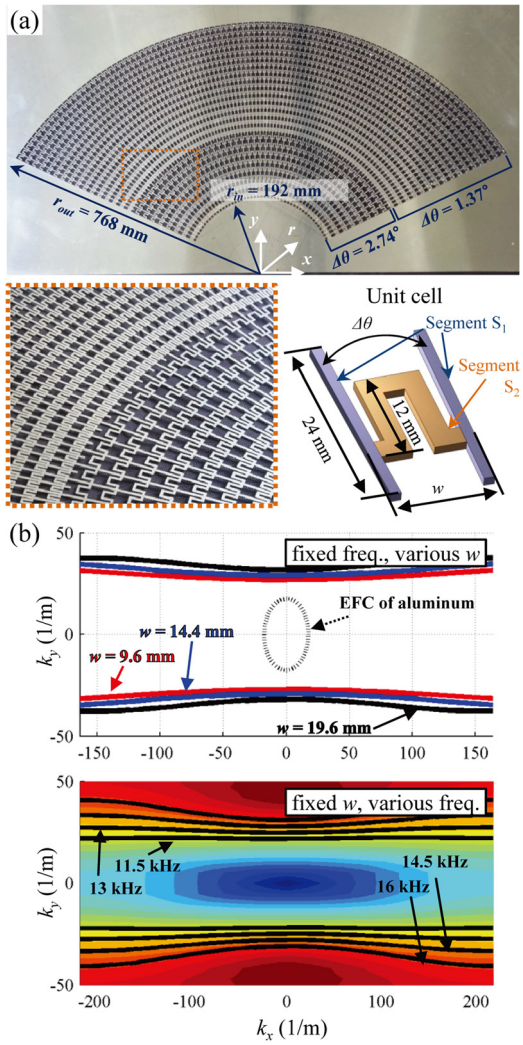

FIG. 3. (a) Photo of the fabricated elastic lens and geometry of the unit cell. (b) (upper) EFCs at 15 kHz for varying values of the width w of the corrugated unit cell in (a), (lower) EFCs for the fixed $w = 14.4$ mm value for varying frequencies.

$\Delta\theta$ at the same radial locations. As we move along the positive radial coordinate, the width w of the unit cell is increased by 1.2 mm but other geometric variables remain unchanged. If w becomes too large in the outer region of the lens, however, the frequency range of hyperbolic EFCs may be quite off from the target frequency. Therefore, a little trick is used; if w becomes larger than $w^* = 19.2$ mm, the unit cell is divided into two smaller unit cells for which w and $\Delta\theta$ are reduced by half. This means that the resulting unit cells from that location grow from $w = w^*/2 = 9.6$ mm incrementally by 0.6 mm with $\Delta\theta = 1.37°$. Thus, w varies from 9.6 mm to 19.2 mm in the whole region of the metamaterial lens fabricated in Fig. 3(a). Numerical simulations showed that the overall wave phenomenon is virtually unaffected by this modification.

The magnification ratio, i.e., the ratio between the inner radius and the outer radius of the fabricated metamaterial lens, is 1:4, but a higher magnification ratio can be realized if one adds more unit cells. Finally, we compare the wavelength (λ) of the lowest symmetric Lamb wave mode (usually known as the S0 mode) propagating in a homogeneous 1-mm thick aluminum plate with the unit cell size. Because $\lambda = 346.66$ mm at 15 kHz, the wavelength is

approximately 14 times larger than the length of the longest side in the unit cell (24 mm—see Fig. 3(a)). Since the fabricated unit cells are sufficiently small compared with the wavelength, multiple refractions of the transmitted waves[17] in the lens may be insignificant.

The hyperbolic nature of the EFCs for the fabricated metamaterial lens should be checked and the results are plotted in Fig. 3(b). Because $\Delta\theta$ is very small, the behavior of the unit cell can be accurately predicted by an equivalent rectangular unit cell defined in the Cartesian coordinate system. Recalling that the widths (w) of the unit cells in the metamaterial lens vary from the minimum value of 9.6 mm to the maximum value of 19.2 mm in the lens, Fig. 3(b) shows the EFCs at the target frequency of 15 kHz for $w = 9.6$ mm, 14.4 mm, and 19.2 mm. The results were calculated by the finite element analysis[25] with the following material properties: ρ (density) $= 2700\,\mathrm{kg/m^3}$, c_l (longitudinal wave speed) $= 5394\,\mathrm{m/s}$, and c_t (transverse wave speed) $= 3122\,\mathrm{m/s}$ for aluminum and $\rho = 1\,\mathrm{kg/m^3}$, $c_l = 330\,\mathrm{m/s}$, and $c_t = 0\,\mathrm{m/s}$ for air. The plots in Fig. 3(b) confirm that the hyperbolic EFCs are apparent for a wide range of w's. It is also important to make sure that the working frequency is not too narrow (as may be the case in metamaterials using resonances). Fig. 3(b) also presents EFCs for varying frequencies near the target frequency for a fixed value of $w = 14.4$ mm. The hyperbolic nature of the resulting EFCs is apparent from Fig. 3(b).

Perhaps, the evaluation of effective parameters for elastic metamaterials helps to explain analytically the hyperbolic nature demonstrated in Fig. 3(b). However, the estimation of the effective stiffness tensors (such as C_{rrrr}, $C_{rr\theta\theta}$, $C_{\theta\theta\theta\theta}$, $C_{\theta\theta r\theta}$, $C_{r\theta r\theta}$) in the elastic case even with an assumption of scalar density field (ρ) appears to require further extensive work because currently available methods developed for acoustic and electromagnetic metamaterials involving vector quantities cannot be directly applied. Nevertheless, the results obtained by the finite element analysis reveal the hyperbolic nature of the proposed elastic metamaterial.

Before presenting experimental verification for sub-wavelength imaging, some simulations are performed to show performance improvement in comparison with the elliptic EFCs. For the comparison, we will take the elastic lens having elliptic EFCs[12] for sub-wavelength imaging. For harmonic-wave simulations performed with COMSOL Multiphysics,[26] two sub-wavelength sources are located within half the wavelength (λ) at the frequency of 15 kHz and the results are presented in Figs. 4(a)–4(c). While the lens having elliptic EFCs is capable of sub-wavelength imaging, higher-resolution by the proposed hyperlens is apparent as compared in Fig. 4; as the distance between the two sources is reduced, the better performance of the lens having hyperbolic EFC becomes evident. Further numerical simulations (before meshing problems occur) show that the proposed hyperlens can separate two sources having the minimum distance of $\lambda/10$, a sub-wavelength distance that is not possibly distinguished by the elastic hyperlens previously proposed.[12] Because the hyperlens in Ref. 12 was based on an elliptic EFC, some sub-wavelength information is lost in a far-field. On the other hand, the hyperlens proposed in this work is based on a hyperbolic EFC so that sub-wavelength information can be considerably better carried.

In Fig. 5, we present experimental results obtained by the fabricated metamaterial lens. The experiments were performed at 15 kHz for which the lowest symmetric S0 Lamb wave mode was dominantly excited in the aluminum plate. The widths of the two line sources, as indicated in Fig. 5(a), are 150 mm (corresponding to 0.43λ). The distance between the centers of the two sources was set to be 167 mm that corresponds to 0.48λ. To realize the S0 wave line sources of 150 mm in width, special magnetostrictive transducers[27] were employed; the transducer was so designed as to actuate five vertically arranged magnetostrictive patches simultaneously,

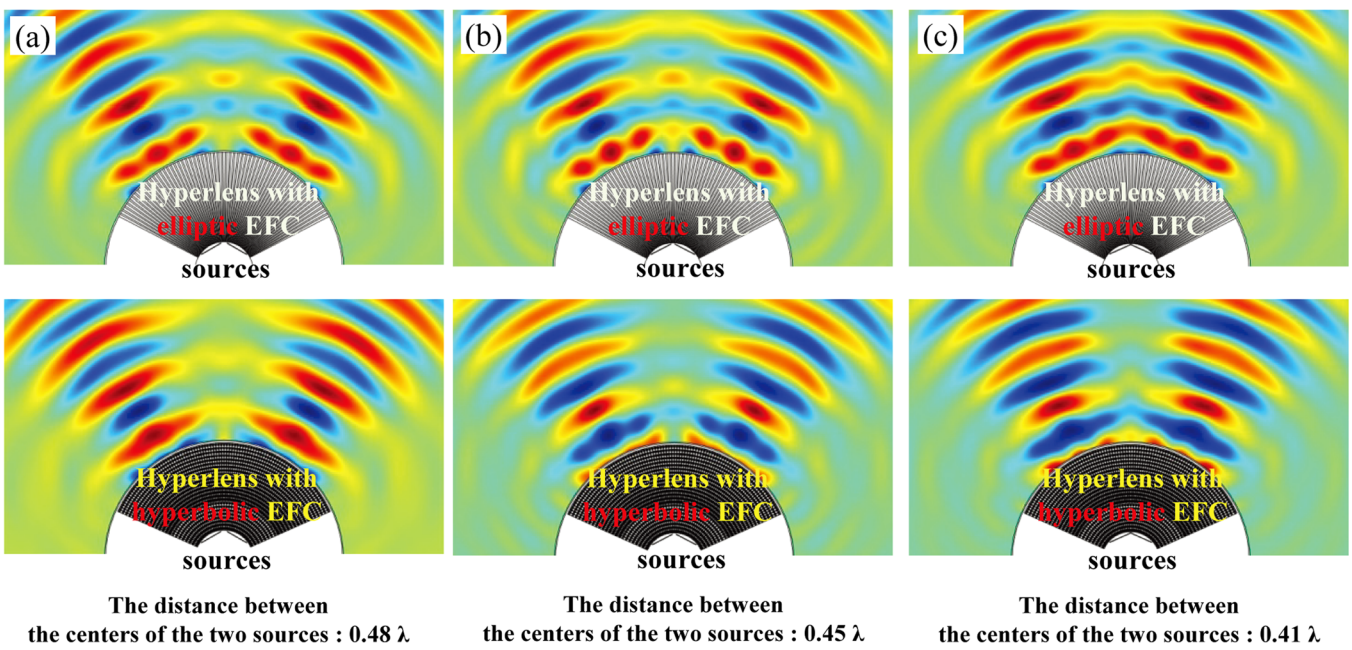

FIG. 4. Performance comparison of the hyperlenses having hyperbolic and elliptic EFCs with the two sub-wavelength sources of which the distance are (a) 0.48 λ, (b) 0.45 λ, and (c) 0.41 λ.

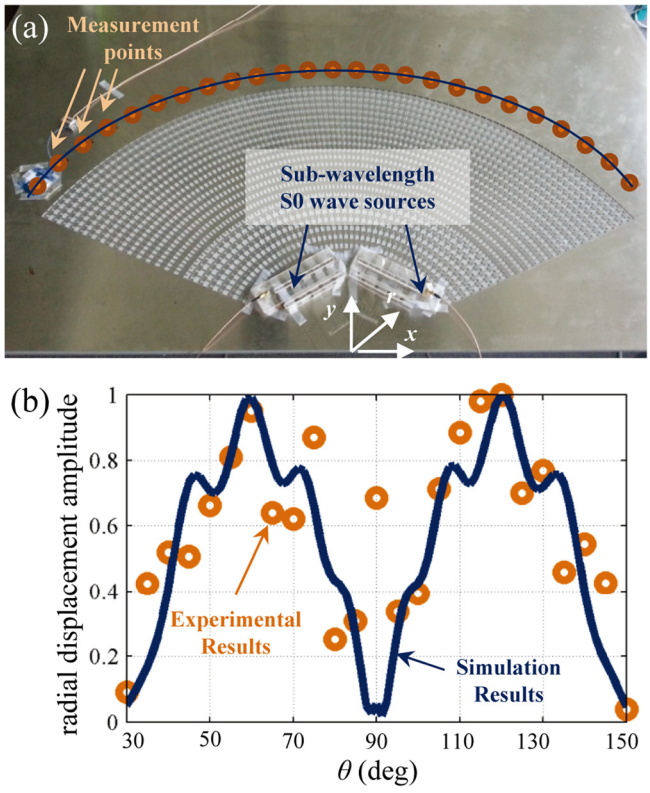

FIG. 5. (a) Photo of the experimental setup with the elastic lens exhibiting truly hyperbolic EFCs. (b) Comparison of the numerical and experimental results of the radial displacement at the measurement points.

each of which is 30 × 30 × 0.15 mm in size. They were placed very near to the inner radius of the metamaterial lens. The modulated Gaussian pulse centered at 15 kHz was used as the actuation pulse signal. The transmitted S0 waves through the metamaterial lens were measured by the square magnetostrictive transducers.[28] Measurements were made at 25 points with an increment of $\theta = 5^\circ$ from 30° to 150° for the fixed value of $r = 850$ mm that is measured from the origin of the lens. Measured time signals were post-processed by the short-time Fourier transformation and the frequency components of 15 kHz were extracted and plotted in Fig. 5(b).

Fig. 5(b) shows good agreements between the experimental and numerical results. The results in Fig. 5(b) suggest that simulations by the finite element calculation are sufficiently accurate and thus the simulated higher-resolution by the proposed hyperlens over the previous one[12] is indeed confirmed indirectly.

The diffraction limit can be broken with elliptic EFCs, but with hyperbolic EFCs, one can go further beyond the current limited resolution realized elliptic EFCs. It is recalled that all earlier attempts in elastic field have so far realized metamaterial lenses exhibiting elliptic EFCs only. Thus, it was natural for us to raise a fundamental question: *"Is the realization of an elastic metamaterial lens exhibiting hyperbolic EFC possible?"* Through this study, we actually developed a unique corrugated elastic metamaterial lens that realizes hyperbolic EFCs. The hyperbolic EFCs were realized by imposing different mechanical deformation modes in two orthogonal directions: dominant extensional deformation in the radial propagating direction and dominant bending deformation in the circumferential non-propagation direction. In spite of some limitations in the present realization, such as low operating frequency range and transmission, the hyperbolic EFC characteristics by the proposed elastic metamaterial were verified by experiments. Simulations clearly showed that much high-resolution difficult or impossible to be realized with an elastic lens of elliptic EFCs can be indeed attained with the proposed metamaterial lens of hyperbolic EFCs.

This work was supported by the National Research Foundation of Korea (NRF) Grant (No: 2013-035194 and 2013-055323) funded by the Korean Ministry of Education, Science and Technology (MEST) contracted through IAMD at Seoul National University.

[1]Z. Jacob, L. V. Alekseyev, and E. Narimanov, Opt. Express **14**, 8247 (2006).
[2]A. Salandrino and N. Engheta, Phys. Rev. B **74**, 075103 (2006).
[3]Z. Liu, H. Lee, Y. Xiong, C. Sun, and X. Zhang, Science **315**, 1686 (2007).
[4]H. Lee, Z. Liu, Y. Xiong, C. Sun, and X. Zhang, Opt. Express **15**, 15886 (2007).
[5]A. Kildishev and E. Narimanov, Opt. Lett. **32**, 3432 (2007).
[6]W. Wang, H. Xing, L. Fanb, Y. Liu, J. Ma, L. Lin, C. Wang, and X. Luo, Opt. Express **16**, 21142 (2008).
[7]J. Rho, Z. Ye, Y. Xiong, X. Yin, Z. Liu, H. Choi, G. Bartal, and X. Zhang, Nat. Commun. **1**, 143 (2010).
[8]T.-Y. Chiang, L.-Y. Wu, C.-N. Tsai, and L.-W. Chen, Appl. Phys. A **103**, 355 (2011).
[9]J. Li, L. Fok, X. Yin, G. Bartal, and X. Zhang, Nature Mater. **8**, 931 (2009).
[10]P. Sheng, Nature Mater. **8**, 928 (2009).
[11]X. Ao and C. T. Chan, Phys. Rev. E **77**, 025601 (2008).
[12]H. J. Lee, H. W. Kim, and Y. Y. Kim, Appl. Phys. Lett. **98**, 241912 (2011).
[13]D. Lu and Z. Liu, Nat. Commun. **3**, 1205 (2012).
[14]C. Ma, R. Aguinaldo, and Z. Liu, Chin. Sci. Bull. **55**, 2618 (2010).
[15]M. S. Kushwaha, P. Halevi, L. Dobrzynski, and B. Djafari-Rouhani, Phys. Rev. Lett. **71**, 2022 (1993).
[16]L. Brillouin, *Wave Propagation in Periodic Structures* (Dover Publications, Inc., NY, 1946).
[17]M. H. Lu, C. Zhang, L. Feng, J. Zhao, Y. F. Chen, Y. W. Mao, J. Zi, Y. Y. Zhu, S. N. Zhu, and N. B. Ming, Nature Mater. **6**, 744 (2007).
[18]Y. Lai, Y. Wu, P. Sheng, and Z. Q. Zhang, Nature Mater. **10**, 620 (2011).
[19]J. Christensen and F. J. Garcia de Abajo, Phys. Rev. Lett. **108**, 124301 (2012).
[20]See supplementary material at http://dx.doi.org/10.1063/1.4865907 for the detailed analysis of the mass-spring system.
[21]Y. Y. Kim and H. C. Lee, Int. J. Solids Struct. **38**, 1327 (2001).
[22]Z. Liang and J. Li, Phys. Rev. Lett. **108**, 114301 (2012).
[23]Y. Xie, B.-I. Popa, L. Zigoneanu, and S. A. Cummer, Phys. Rev. Lett. **110**, 175501 (2013).
[24]Z. Liang, T. Feng, S. Lok, F. Liu, K. B. Ng, C. H. Chan, J. Wang, S. Han, S. Lee, and J. Li, Sci. Rep. **3**, 1614 (2013).
[25]P. Langlet, A.-C. Hladky-Hennion, and J.-N. Decarpigny, J. Acoust. Soc. Am. **98**, 2792 (1995).
[26]COMSOL Multiphysics, *COMSOL Multiphysics Modeling Guide: Version 3.5* (COMSOL AB, Stockholm, 2008).
[27]J. H. Oh, H. W. Kim, P. S. Ma, H. M. Seung, and Y. Y. Kim, Appl. Phys. Lett. **100**, 213503 (2012).
[28]J. S. Lee, S. H. Cho, and Y. Y. Kim, Appl. Phys. Lett. **90**, 054102 (2007).